

# A Numerical Study on the Interaction Between Different Position of Cellular Headsets and a Human Head

R. Aminzadeh<sup>1,2</sup>, A. Abdolali<sup>2</sup>, and H. Khaligh<sup>3</sup>

<sup>1</sup>School of Engineering and Science,  
Sharif University of Technology-International Campus, Kish Island, 79417-76655, Iran  
aminzadeh@kish.sharif.edu

<sup>2</sup>Bioelectromagnetics Research Group, Department of Electrical Engineering,  
Iran University of Science and Technology, Tehran, 1684613114, Iran  
abdolali@iust.ac.ir

<sup>3</sup>Department of Electrical and Computer Engineering,  
University of Waterloo, Waterloo, N2L-3G1, Canada  
h8hossei@uwaterloo.ca

**Abstract** — In this paper the interaction between a human head exposed to a bluetooth-based cellular headset in different positions is studied. The exposure to the electromagnetic fields is a concern when people use these devices. The interaction of human head and bluetooth mobile headsets has not been considered in related standards. In this research three installed positions for the headset and two scenarios for the user are defined. In the first scenario the user is in free space and in the second scenario the user is in a car. For both scenarios path loss, antenna gain, total isotropic sensitivity, and specific absorption rate values for three positions of the headset on the head are obtained. SEMCAD X software is used as an FDTD-based simulation platform for our numerical studies. The result of our study can help manufacturers to consider the compatibility of these devices with safety guidelines of electromagnetic exposure specified by relevant institutes. Designers of wireless devices can use results of this study to design new headsets that can be used in an appropriate position while the performance of the device is less affected by the human head and the environment.

**Index Terms** - Bluetooth, electromagnetic field, FDTD, headset, human head, and SEMCAD.

## I. INTRODUCTION

Telecommunication technologies attract more users each day and spread all over the world. Cellular phones are a part of this technology that attract users from all different age groups. The continuous growth of high-end devices forces companies to ensure their new products to be compatible with safety guidelines specified by related standards like IEEE Standard-1528 [1] and International Electrotechnical Commission, IEC 62209-1 [2]. Bluetooth headsets are one of applications that communicate to the cellular phone via bluetooth protocol [3] at 2400 MHz-2450 MHz frequency range. The question is that: *Is user head exposure to bluetooth headsets safe?* To answer this question we aim to evaluate the interaction between a human head exposed to a bluetooth-based cellular headset. Several headset models are produced with different specifications. Each product has a different effect on the user head based on its antenna type, operation frequency, housing, case material, and installed position.

SAR measurement of a human head exposed to a bluetooth headset has not been considered in related standards [1, 2, 4-9]. This is while the interaction between human body and wireless devices has been an interesting subject of studies over the past sixteen years [10-15]. The effect of

human hand on antenna characteristics of cellular handsets such as total radiated power and far field behavior was studied in [10]. The effect of human body on implantable antennas was inspected in [11-13]. In [14] SAR computation and temperature distribution in human body has been investigated.

In [15] numerical analysis of the interaction between human head and cellular phones has been performed by modeling the phone as a metal box with an antenna inside or outside the box. In [16] authors have studied the effect of different case materials on induced SAR in a human head.

In this paper the finite-difference time-domain (FDTD) method is used because it is simpler and easier to implement, compared with the finite element method (FEM). Despite computational implementation, FDTD is used for easy comparison of our results with SAR measurement standards, which have been developed based on FDTD method (cf. [1, 2]). SEMCAD X software [17], an FDTD-based platform, is chosen due to its user friendly interface and capability of 3D-model analysis.

This paper is organized as follows: section II is a description of designed headset model; human head, car, and antenna models. Section III includes explanation of settings and configurations as well as grid generation. Section IV, presents the simulation results for path loss, antenna gain, total isotropic sensitivity, and specific absorption rate and a comparison of proposed scenarios and finally section V concludes the paper.

## II. MODELING

### A. Mobile headset

To study the interaction between mobile headsets and human head, a mobile headset model is designed based on real ones usually found at the market. To obtain more accurate results the effect of case material is also considered. In this paper acetal is considered as the case material for the mobile headset, it is used for the case material in mobile phone accessories [18]. Figure 1 shows the headset model. In the rest of the paper the term headset is used instead of mobile headset.

### B. Human head

Because of the dependency of electrical properties of human head on frequency a dispersive model, SAM (specific anthropomorphic

mannequin) phantom is used for a conservative estimate of SAR in compliance with international exposure standards. SAM is a simplified and homogeneous model of human head that contains SAM shell and liquid. SAM shell is a lossless plastic shell filled with a homogeneous liquid that has electrical properties of head tissue and has an ear spacer. Parameters of this phantom are different from the model introduced by IEEE standard committee (SCC34/SC2/WG1) [19]. The dielectric properties (relative permittivity and electrical conductivity) of SAM phantom [1] and acetal [18] at 2400 MHz – 2450 MHz are extracted and listed in Table 1. As SAM is a homogeneous model relative permittivity and conductivity values are considered. Headset is installed on the left ear at 30°, 52°, and 60°, which are three most common positions. SAM phantom with the headset at the angle of 30° is called model 1. Model 2 is referred to the position of headset at the angle of 52° and model 3 is the chosen name for headset, which is rotated by 60°. Two scenarios are considered for these three models; the first scenario is the situation where each model is simulated in free space. In the second scenario to study the effect of metal and dielectric parts, i.e., complex environments, each model is simulated while the user is in a car.



Fig. 1. Designed headset model.

Table 1: Dielectric properties of SAM phantom and acetal at 2400 MHz – 2450 MHz.

Material	$\delta$ (s/m)	$\epsilon_r$
SAM shell	0.0016	5
SAM liquid	1.8	39.2
acetal	0.002	2.8

Figure 2 shows SAM phantom and the headset installed at the angle of 60° (model 3); blue lines indicate the position of the headset in models 1 and 2.

### C. Car model

A Ferrari, which is available in SEMCAD X software is chosen as the car model. Car seats, dashboard, glass, tires, and lights are assumed as dielectric parts. Other parts like body, chassis, wheels, door, hood, and brakes are considered as perfect electric conductor (PEC) parts. Figure 3 depicts the user inside the car model.

### D. Antenna model

For bluetooth communications a planar inverted F-antenna (PIFA) is used in SEMCAD X. It operates at the range of 2400 MHz – 2450 MHz. A sinusoidal voltage source with a resistance of 50 ohm is used as the excitation source at the antenna feed point. This antenna has a coaxial feed point with the length of 1.8 mm and diameter of 0.2 mm. Figure 4 shows antenna configurations for the frequency range of 2400 MHz to 2450 MHz. Antenna parameters are also described in Table 2.

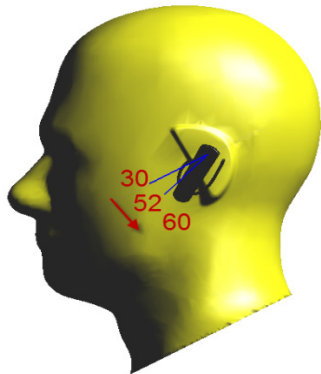


Fig. 2. SAM phantom and the installed headset at three positions.



Fig. 3. Car model and the user inside.

## III. FDTD CONFIGURATION

A minimum spatial resolution of  $2.0 \times 2.0 \times 2.0 \text{ mm}^3$  and a maximum spatial resolution of  $5.0 \times 5.0 \times 5.0 \text{ mm}^3$  is set in the x, y, and z directions.

The baseline resolution should be selected small enough to prevent ignoring certain baselines. It should also be noticed that selecting too small baseline resolution will result in smaller simulation time step and longer simulation time. As the wavelength is 124.91 mm so the minimum baseline resolution is set to  $0.002 \lambda$  (0.24982 mm). The maximum step is usually set to approximately  $\lambda/10$  as a rule-of-thumb [17]. But here to reduce dispersion errors produced automatically by using a non-uniform grid we choose the maximum step as  $\lambda/14$  ( $0.07\lambda$ ), which is equal to 8.7437 mm. The amount of generated FDTD-grid cells for model 1, 2, and 3 are 5.969 M cells ( $185 \times 135 \times 239$ ) for the first scenario (free space) and 57.027 M cells ( $590 \times 319 \times 303$ ) for the second scenario (car). In order to achieve a steady state condition, simulation time is set to 15 sinusoidal periods and total number of 2000 time steps with  $\Delta t = 3.33 \text{ ps}$  is considered. To prevent over-refinement in neighboring cells the maximum ratio of the length of neighboring cells (grading ratio) is set as 1.2 and grading ratio relaxation of 10% is selected to increase the dynamics of the gridded. Refining factor is 10 for all solid regions. The absorbing boundary conditions (ABC) is set as uniaxial perfectly matched layer (U-PML) with 10 layers thickness where the minimum level of absorption at the outer boundary is greater than 99.9%. A bounding box with a refinement in both upper and lower boundary of 0.06 for z-axis is also made for the antenna. The total simulation time was 14 minutes and 85 minutes for free space and the car, respectively (using a computer with core 2 quad CPU and 4 gigabytes of memory).

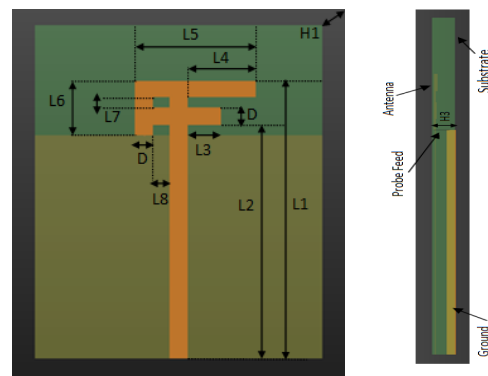


Fig. 4. Antenna configuration for the operation frequency of 2400 MHz – 2450 MHz.

Table 2: Antenna parameters.

Parameter	Length (mm)	Parameter	Length(mm)
L1	50	L5	21
L2	41.95	L6	10
L3	5.9	L7	1.95
L4	11.9	L8	3
D	3.05	H1	0.1

## IV. RESULTS AND DISCUSSION

### A. Path loss

We extract the simulation results for E-field and plot them in MATLAB<sup>TM</sup> software. The results are depicted in Figs. 5 and 6 for three models in both environments. The horizontal axis shows the distance that the E-field passes through the head from the left ear and the vertical axis shows the E-field strength in dB. These values are listed in Table 3. From the results it can be seen that the obtained path loss values for human head inside the car are lower than the free space due to the metal parts (frame) of the car that might serve as a shield and minimize the radiated energy, which results in an increase of E-field. As the headset angle increases, the path loss values for three models decreases in both scenarios. In other words by changing the position of the headset from 30° to 60°, the electric field drops to zero at a longer length. In model 2 the E-field has two lobes and is different from models 1 and 3. The reason is that at the angle of 52° the antenna is closer to the tissues that have high amount of water such as mouth and nose that attenuates the electric field for a short distance in the middle of the field path in the head because of their shape. The minimum path loss values (maximum E-field) are obtained for model 3 inside the car and free space. Computed maximum values of path loss are for model 1 in both scenarios.

### B. Antenna gain

Simulated antenna gain for three models inside the car and free space were obtained and listed in Table 4. In free space by changing the headset position from model 1 to 3, gain value decreases. As the headset position changes from 30° to 60°, antenna radiation power decreases due to the reflection of some parts of radiated waves by the head. When the user is inside the car,

antenna gain decreases more than free space because of radiated wave's reflection by metal parts in the car. Maximum gain value is obtained for model 1 (2.25 dBi) in free space and for model 2 (-5.42 dBi) inside the car. The antenna gain for models 1 and 2 are better than model 3 in free space. It can also be stated that the antenna gain is affected by the glass inside the car that absorbs more power than other dielectric parts as it is closer to the headset.

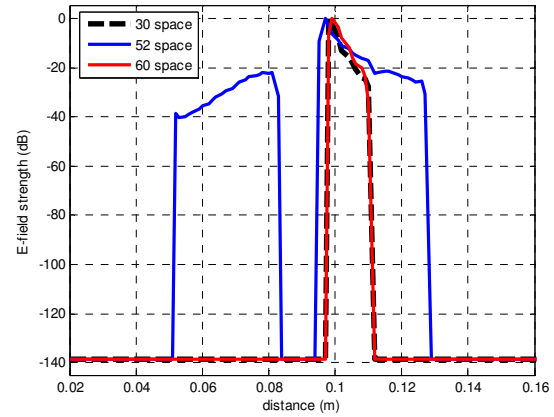


Fig. 5. Path loss simulations in free space; installation degrees are 30°, 52°, and 60°.

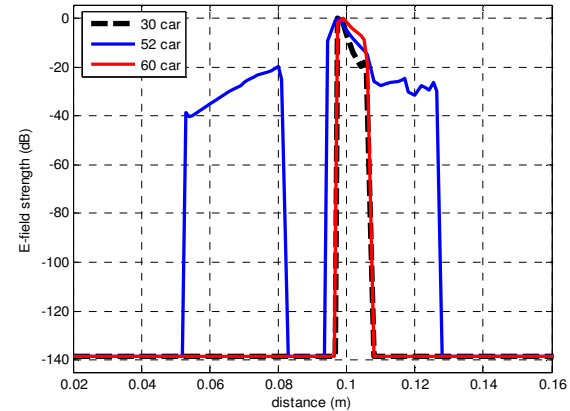


Fig. 6. Path loss simulations in car; installation degrees are 30°, 52°, and 60°.

Table 3: Simulated path loss values in dB.

Model	Model 1	Model 2	Model 3
Position	30°	52°	60°
Free Space	24.2	21.8	20.1
Car	20.8	19.3	9.6

Table 4: Simulated gain values in dBi.

Model	Model 1	Model 2	Model 3
Position	30°	52°	60°
Free Space	2.25	-2.40	-3.08
Car	-5.81	-5.42	-10.45

### C. Total isotropic sensitivity

Total isotropic sensitivity (TIS) is a parameter used to determine the receiving performance and the efficiency of a wireless device. For a bluetooth-based headset TIS can be related to the maximum distance from the cellular phone at which the headset can operate well. Antenna gain, antenna mismatch, and noise can affect TIS. Table 5 describes simulated TIS values for three models inside the car and free space. As it can be seen in Table 5 the value of TIS in model 3 decreases compared with 1 and 2 while the user is in free space. When the headset position changes from model 1 to 3 in free space, the headset (antenna) interacts with more parts of the head and the impedance increases. In the car, the head impedance in model 2 is smaller than 1 and 3 and the best TIS value is obtained for model 2. On the other hand, for model 1 in the car the headset antenna is closer to the roof's foam and in model 3 the antenna is closer to the seats so a part of the transmitted energy is absorbed by these dielectrics in the car and results in fewer TIS.

### D. SAR

In SAR computation by FDTD, the electric field components at the voxel edges are computed in the x, y, and z directions. SAR is defined as follows,

$$SAR = \frac{\sigma_E}{\rho} |E|^2, \quad (1)$$

where  $\sigma_E$  and  $\rho$  are the electric conductivity and mass density of the tissue, respectively, and  $E$  is the electric field. SEMCAD X software supports spatial peak SAR measurement defined by IEEE standard-1529 [9].

Antenna input power is set to 0.0025 W as the maximum radiation power for the second class bluetooth devices (headsets) in 2.4 GHz frequency range. Table 6 describes the results of SAR numerical measurements for three models in free space and inside the car. Based on the results the maximum value of SAR<sub>1g</sub> is for model 1 in free

space (0.1228 W/Kg) and is for model 2, inside the car (0.1153 W/Kg). The maximum value of SAR<sub>10g</sub> in free space and inside the car belongs to model 2, 0.0458 W/Kg and 0.0486 W/Kg, respectively. It can be seen that SAR values inside the car are higher than SAR values in free space. As mentioned in section IV A, this is due to the metal frame of the car that might serve as a shield and minimize the radiated energy, which results in an increase of SAR. The results show that the SAR<sub>1g</sub> and SAR<sub>10g</sub> reach their minimum values for model 3 in free space and inside the car. As mentioned before, model 3 is closer to the seats and more energy is absorbed by the seats, so the SAR value decreases for model 3 compared with 1. All the results are lower than 0.123 W/Kg while due to IEEE C95.1-2005 standard the spatial peak SAR limit in USA is 1.6 W/Kg per 1g tissue and for Japan and European countries it is 2 W/Kg per 10 g tissue [20].

Table 5: Simulated TIS values in dBm.

Model	Model 1	Model 2	Model 3
Position	30°	52°	60°
Free Space	-56.32	-45.05	-38.26
Car	-30.90	-33.31	-26.71

Table 6: Averaged SAR<sub>1g</sub> and SAR<sub>10g</sub> values in human head for three models in free space and the car.

Free Space			
Model	Model 1	Model 2	Model 3
Position	30°	52°	60°
SAR <sub>1g</sub> in head	0.1228	0.1075	0.0535
SAR <sub>10g</sub> in head	0.0455	0.0458	0.0203
Car			
Position	30°	52°	60°
SAR <sub>1g</sub> in head	0.0967	0.1153	0.0818
SAR <sub>10g</sub> in head	0.0358	0.0486	0.0287

It is concluded that the safer model is model 3 that has the least SAR values both in free space and inside the car. Figures 7 and 8 show the slice field distribution of SAR 1g and 10g values for three models inside the car and free space, respectively. It can be seen that in model 1 the peak spatial SAR occurs at a higher region and closer to the ear compared with model 3.

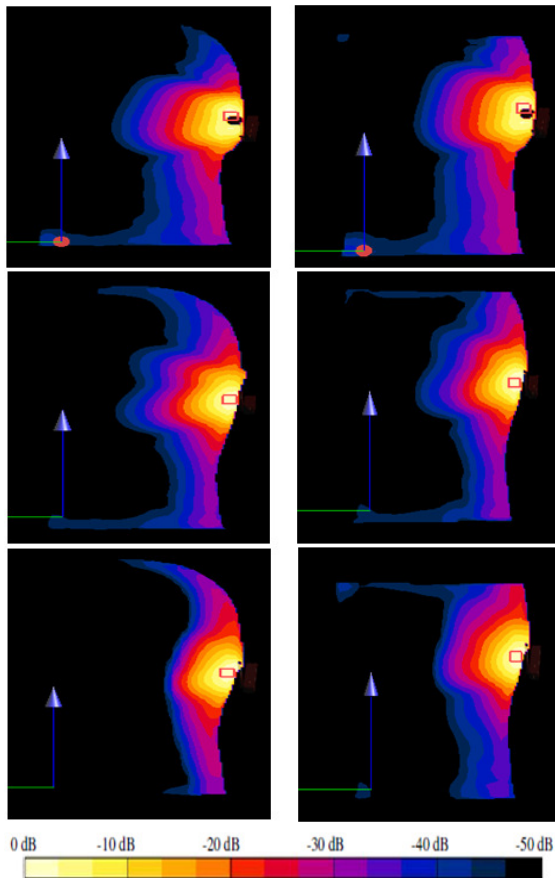


Fig. 7. Slice distribution of spatial peak SAR averaged over 1g for model 1, 2, and 3 (from top to bottom) in free space (left column) and inside the car (right column).

## V. CONCLUSION

In this paper the interaction between a mobile headset and the human head was modeled and simulated. A mobile headset was designed and SAM phantom was used as a homogeneous head model. Three positions were defined for the mobile headset. A PIFA was used as a suitable antenna for bluetooth communications. Two scenarios where the user is in free space and inside the car were described. SEMCADX software was used as an FDTD-based simulation platform for our numerical studies. Finally, we discussed and obtained results for path loss, antenna gain, TIS, and SAR. Based on our results the best model in the proposed research was model 3, which had the minimum SAR values for both scenarios where the user was inside the car and in free space. Due to low radiation power of the antenna, a large part

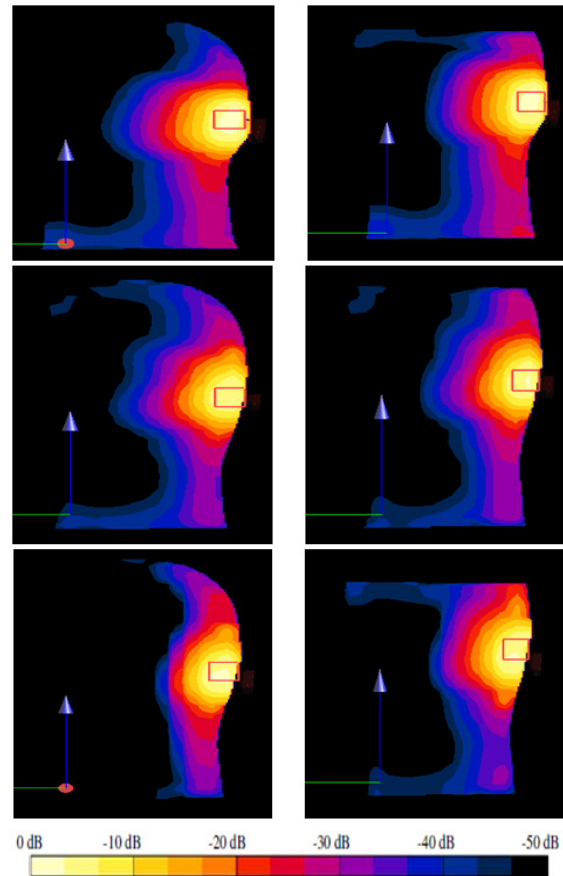


Fig. 8. Slice distribution of spatial peak SAR averaged over 10g for model 1, 2, and 3 (from top to bottom) in free space (left column) and inside the car (right column).

of the electric field was absorbed by dielectric parts or was reflected by metal parts in the car. This was while model 3 had the worst antenna gain in the car. The result of our study can help manufacturers to consider the compatibility of these devices with safety guidelines of electromagnetic exposure specified by relevant institutes. Designers of wireless devices can also use these results to design new headsets that can be used in an appropriate position while the performance of the device is less affected by the human head and the environment.

## ACKNOWLEDGMENT

The authors would like to thank Schmid and Partner Engineering AG (SPEAG) for providing the license for SEMCADX software through *SEMCAD X for Science* agreement. In addition the

authors wish to thank Dr. K. Hajsadeghi from Sharif University of Technology for proof reading the paper and M. Ashiri and Marjan Joorabchi, M.Sc. students at Sharif University of Technology-International Campus, for their helpful comments on preparing the final draft of this paper.

#### REFERENCES

- [1] IEEE Recommended Practice for Determining the Peak Spatial-Average Specific Absorption Rate (SAR) in the Human Head from Wireless Communications Devices: Measurement Techniques, IEEE Standard-1528, Dec. 2003.
- [2] Standard, "Human exposure to radio frequency fields from hand-held and body-mounted wireless communication devices — Human models, instrumentation, and procedures — Part 1: Procedure to determine the specific absorption rate (SAR) for hand-held devices used in close proximity to the ear (frequency range of 300 MHz to 3 GHz)," IEC 62209-1, 2006.
- [3] IEEE 802.15 Working Group for WPAN. Available online: <http://www.ieee802.org/15/>.
- [4] Standard, "Product Standard to Demonstrate the Compliance of Mobile Phones with the Basic Restrictions Related to Human Exposure to Electromagnetic Fields (300 MHz – 3 GHz)," European Committee for Electrical Standardization (CENELEC), EN 50360, Brussels, 2001.
- [5] Standard, "Basic Standard for the Measurement of Specific Absorption Rate Related to Exposure to Electromagnetic Fields from Mobile Phones (300 MHz – 3 GHz)," European Committee for Electrical Standardization (CENELEC), EN 50361, Brussels, 2001.
- [6] Standard, "Specific Absorption Rate (SAR) Estimation for Cellular Phone," ARIB Standard-T56, 2002.
- [7] Standard, "Evaluating Compliance with FCC Guidelines for Human Exposure to Radio Frequency Electromagnetic Fields," supplement C to OET Bulletin 65 (Edition 9701) FCC, 1997.
- [8] Standard, "Electromagnetic Radiation - Human Exposure," ACA Radio Communications Standard, Schedules 1 and 2, 2003.
- [9] Standard, "IEEE standard, Recommended Practice for Determining the Peak Spatial-Average Specific Absorption Rate (SAR) associated with the use of wireless handsets- computational techniques," IEEE-1529, draft standard.
- [10] J. Krogerus, J. Toivanen, C. Icheln, and P. Vainikainen, "Effect of the human body on total radiated power and the 3-D radiation pattern of mobile handsets," *IEEE Trans. Instrum. Meas.*, vol. 56, no. 6, Dec. 2007.
- [11] J. Gemio, J. Parron, and J. Soler, "Human body effects on implantable antennas for ISM bands applications: models comparison and propagation losses study," *Progress In Electromagnetics Research*, vol. 110, pp. 437-452, 2010.
- [12] N. Vidal, S. Curto, J. M. Villegas, J. Sieiro, and F. M. Ramos, "Detuning study of implantable antennas inside the human body," *Progress In Electromagnetics Research*, vol. 124, pp. 265-283, 2012.
- [13] H. Virtanen, J. Huttunen, A. Toropainen, and R. Lappalainen, "Interaction of mobile phones with superficial passive metallic implants," *Phys. Med. Biol.*, vol. 50, no. 26892700, 2005.
- [14] T. Wessapan, S. Srisawatdhisukul, and P. Rattanadecho, "Specific absorption rate and temperature distributions in human head subjected to mobile phone radiation at different frequencies," *International Journal of Heat and Mass Transfer*, vol. 55, no. 347359, 2012.
- [15] M. Okoniewski and M. Stuchly, "A study of the handset antenna and human body interaction," *IEEE Trans. Microw. Theory Tech.*, vol. 44, no. 10, pp. 1855-1864, 1996.
- [16] R. Aminzadeh, M. Ashiri, and A. Abdolali, "SAR computation of a human head exposed to different mobile headsets using FDTD method," *In Proc. Progress In Electromagnetics Research Symposium*, KL, Malaysia, pp. 1131-1134, March 2012.
- [17] SEMCAD X by SPEAG, "Reference Manual for the SEMCAD Simulation Platform for Electromagnetic Compatibility, Antenna Design and Dosimetry," Schmid & Partner Engineering AG (SPEAG), <http://www.speag.com>.
- [18] Y. Cho, S. Hwang, O. Ishida, and S. Park, "Dual band internal antenna of PIFA type for mobile handsets and the effect of the handset case and battery," *In Proc. of IEEE Antennas. Propag. Int. Symposium*, vol. 1A, pp. 487-490, July 2005.
- [19] B. Beard, W. Kainz, T. Onishi, et al., "Comparisons of computed mobile phone induced SAR in the SAM phantom to that in anatomically correct models of the human head," *IEEE Trans. Electromagn. Compat.*, vol. 48, no. 2, pp. 397-407, 2006.
- [20] Standard, "IEEE Standard for Safety Levels with Respect to Human Exposure to Radio Frequency Electromagnetic Fields, 3kHz to 300 GHz, Amendment2: Specific Absorption Rate (SAR) Limits for the Pinna," IEEE Standard C95.1b, 2005.



**Reza Aminzadeh** was born in Iran in 1987. He received his B.Sc. degree in Electrical Engineering in 2010. He is currently working toward the M.Sc. degree in Electrical Engineering at Sharif University of Technology-International Campus. Currently he works as a research assistant at computational electromagnetics laboratory at Sharif University of Technology. Since 2010 he has been with the Bioelectromagnetics research group, at Iran University of Science and Technology (IUST) as a research assistant.

He has been Associate editor of PEAK magazine (National Scientific Student's Organization of Electrical Engineering) from 2011 to 2012. His main research areas are computational electromagnetics, wave propagation modeling in human body, bioelectromagnetics, microwave imaging and tomography. Since 2012 he has been a member of computational electromagnetic technical committee (TC9) of the IEEE EMC society and TC95-subcommittee 4 of international committee on electromagnetic safety (ICES). He served as technical program committee member of IEEE International Conference on Ultra-Wideband (ICUWB) in 2012 and 2013 and also IEEE international symposium on electromagnetic compatibility (EMC 2013).



**Ali Abdolali** was born in Tehran, Iran, on May 3, 1974. He received B.S. degree from the University of Tehran, and M.S. degree from the University of Tarbiat Modares, Tehran, and the Ph.D. degree from Iran University of Science and Technology (IUST), Tehran, Iran, all in Electrical Engineering, in 1998, 2000, and 2010, respectively. In 2010, he joined the Department of Electrical Engineering, Iran University of Science and Technology, Tehran, Iran, where he is an assistant Professor of electromagnetic engineering. His research interests include electromagnetic wave scattering, Radar Cross Section (RCS), Radar Absorbing Materials (RAM), EM Waves controlling, cloaking, metamaterials, EM Waves in complex media (anisotropic, inhomogeneous, dispersive media, metamaterials), Frequency Selective Surfaces (FSS), Bio-electromagnetism (BEM). He has authored or coauthored over 40 papers in international journals and conferences.



**Hadi Hosseinzadeh Khaligh** received his B.Sc. in Materials Engineering at the University of Tehran, Iran. He is currently pursuing his M.Sc. in Nanotechnology in the Department of Electrical and Computer Engineering. His research is focused on the integration of metal nanowires into novel electronic devices.